Journal of Magnetic Resonance 216 (2012) 175–182

Contents lists available at SciVerse ScienceDirect

Journal of Magnetic Resonance

journal homepage: www.elsevier.com/locate/jmr

W-band PELDOR with 1 kW microwave power: Molecular geometry, flexibility and exchange coupling

Gunnar W. Reginsson [a,b], Robert I. Hunter [c], Paul A.S. Cruickshank [c], David R. Bolton [c], Snorri Th. Sigurdsson [b], Graham M. Smith [c,*], Olav Schiemann [a,*]

[a] Biomedical Sciences Research Complex, Centre of Magnetic Resonance, University of St Andrews, St Andrews KY16 9ST, UK
[b] Science Institute, University of Iceland, Dunhaga 3, 107 Reykjavik, Iceland
[c] School of Physics and Astronomy, Centre of Magnetic Resonance, University of St Andrews, St Andrews KY16 9SS, UK

ARTICLE INFO

Article history:
Received 10 November 2011
Revised 9 January 2012
Available online 8 February 2012

Keywords:
PELDOR
DEER
Nitroxide spin labels
Orientation selective PELDOR
Exchange coupling

ABSTRACT

A technique that is increasingly being used to determine the structure and conformational flexibility of biomacromolecules is Pulsed Electron–Electron Double Resonance (PELDOR or DEER), an Electron Paramagnetic Resonance (EPR) based technique. At X-band frequencies (9.5 GHz), PELDOR is capable of precisely measuring distances in the range of 1.5–8 nm between paramagnetic centres but the orientation selectivity is weak. In contrast, working at higher frequencies increases the orientation selection but usually at the expense of decreased microwave power and PELDOR modulation depth. Here it is shown that a home-built high-power pulsed W-band EPR spectrometer (HiPER) with a large instantaneous bandwidth enables one to achieve PELDOR data with a high degree of orientation selectivity and large modulation depths. We demonstrate a measurement methodology that gives a set of PELDOR time traces that yield highly constrained data sets. Simulating the resulting time traces provides a deeper insight into the conformational flexibility and exchange coupling of three bisnitroxide model systems. These measurements provide strong evidence that W-band PELDOR may prove to be an accurate and quantitative tool in assessing the relative orientations of nitroxide spin labels and to correlate those orientations to the underlying biological structure and dynamics.

1. Introduction

Pulsed Electron–Electron Double Resonance (PELDOR or DEER) [1,2] is increasingly being used to determine structures and conformational changes of biologically relevant macromolecules. Using intrinsic paramagnetic centres or site specifically incorporated spin labels into proteins or nucleic acids PELDOR is used to measure the distance between spin centres and to relate distance distributions to conformational states [3–5]. In addition to measuring distances between spin labelled sites, PELDOR can also be used to measure the relative orientation of spin centres [6,7]. Whilst most standard spin labels such as MTSSL are very flexible and known to give a very broad distribution of orientations, new spin labels are now being developed that have less flexibility. Using such rigid spin labels or spin labelling sites with restricted spin label dynamics, orientation-sensitive PELDOR measurements have been demonstrated at X-band frequencies where they have been used to obtain information on relative orientations of spin labels and dynamics. Examples include DNAs spin labelled with the rigid spin label Ç [8–10], the spin labelled potassium ion channel [11] and copper nitroxide biradical model systems [12,13]. The recent development of the so-called RX nitroxide spin label with two linkers [14,15] also gives hope that in the future protein systems may be spin labelled in a rigid way. Performing PELDOR measurements at 94 GHz (W-band) [7,16–18] or 180 GHz (G-band) [6,10,19] gives a much higher orientation resolution since the *g*-tensors become better resolved, but at the same time the PELDOR modulation depth decreases as a result of less microwave power being available with the spectrometers used. An exception is the W-band PELDOR study by the lab of Goldfarb where a modulation depth of ~20% was achieved with 1 W of power [20]. A deep modulation is important since the dipolar information is contained in the modulation rather than the absolute echo height. All the high-field/high-frequency studies mentioned above also used relatively high *Q* single-mode cavities to improve sensitivity, which limited the available instantaneous bandwidth, restricting the frequency separation between inversion and detection pulses. To invert and detect a full set of orthogonal orientations in a PELDOR experiment requires an effective bandwidth of 250–300 MHz, which previously required lowering the *Q*-value of the cavity substantially with a significant loss of sensitivity. One exception is the promising approach described by Bennati et al. where a bimodal cavity was used to provide separate

* Corresponding authors.
E-mail addresses: gms@st-andrews.ac.uk (G.M. Smith), os11@st-andrews.ac.uk (O. Schiemann).

1090-7807/$ - see front matter © 2012 Elsevier Inc. All rights reserved.
doi:10.1016/j.jmr.2012.01.019

tuneable cavity resonances for both inversion and detection pulses, although sensitivity was still limited by the available power [16].

In this work we show that these technical limitations can be overcome and high concentration sensitivity measurements can be made over large bandwidths at 94 GHz. Measurements were made on three bisnitroxide model systems (Fig. 1) using a home-built W-band EPR spectrometer with 1 kW pulse microwave power and a flat 1 GHz instantaneous bandwidth (HiPER) [21] obtaining a detailed picture of their molecular geometry, flexibility and exchange coupling.

2. Results and discussions

Continuous wave-EPR (CW-EPR) spectra were recorded of all three bisnitroxides on HiPER at 110 K (Fig. 2). All three compounds show a typical cw W-band nitroxide spectrum with no discernible splittings due to dipolar- or exchange couplings. Simulating all three spectra yielded *g*-tensor values, ^{14}N hyperfine coupling values and linewidths that where used for the simulations of the PELDOR time traces (see Table 2).

In the standard terminology for nitroxide orientations in a magnetic field the nitroxide is oriented in the *x*-direction when the NO-bond is parallel to the applied magnetic field B_0, in the *y*-direction when B_0 is orthogonal to the *x*-direction but in the plane of the five-membered ring system and in the *z*-direction when B_0 is orthogonal to the ring plane (Fig. 3, inset).

At W-band frequencies the *g*-tensors are sufficiently well resolved that it becomes possible to selectively excite nitroxides with specific orientations. Thus, in an orientation selective PELDOR experiment one excites the "*A*" spins of nitroxides oriented in a particular direction via the detection pulse sequence and then monitors the effect of inverting the "*B*" spins of nitroxides oriented in the same or an orthogonal direction. The overall modulation depth is determined by the fraction of *B* spins that were excited by the inversion pulse. The modulation frequency and its damping contains information on both the distribution of distances between the spins and the distribution in orientations of the interspin vector with respect to B_0. In the study described here, we use six separate PELDOR measurements to correlate *A* and *B* spins with each other that are oriented in either the *x*-, *y*- or *z*-directions with respect to the magnetic field. Thus, we describe six inversion/detection PELDOR correlation measurements in the *XX*, *YY*, *ZZ*, *YX*, *YZ* and *ZX* directions, where for example *ZX* means that we invert the spins oriented in the *z*-direction and detect spins oriented in the *x*-direction. It is our experience that this measurement methodology gives a highly constrained data set that can be obtained in about 3 h with the described samples and instrumentation.

An echo detected field swept spectrum of each bisnitroxide was used to guide the positioning of the detection and inversion pulses (Fig. 3). Since HiPER works in reflection mode (without a cavity), it is not limited by a cavity band-width and thus allows one to position inversion and detection pulses at any position on the nitroxide spectrum. This enables one to monitor not only *XX*, *YY* and *ZZ* correlations but also the cross-correlations *XY*, *XZ* and *YZ* with large frequency offsets between inversion and detection, e.g. 210 MHz for *XZ*.

For each of these six inversion/detection combinations a PELDOR time trace was recorded for each of the three biradicals (Fig. 4a, d, and g). The high sensitivity and high microwave power of the HiPER spectrometer allowed the acquisition of each time trace with an average signal to noise (*S*/*N*) ratio of 100 and modulation depths as large as 40% in about 30 min. This modulation depth is close to the 50% obtained at X-band [13,22] and considerably larger than the largest modulation depth of 6% for W-band PELDOR on a power–upgraded Bruker Elexsys 680 spectrometer using either a single or dual mode cavity [7,16] and still larger than the modulation of 20% achieved by Goldfarb et al. [20]. Although, it should be kept in mind that the observed PELDOR modulation depth depends also on the relative orientation and degree of correlation between the coupled spin centres. A quantitative analysis of the three sets of time traces are detailed below.

2.1. Biradical **1**

The set of PELDOR time traces acquired for **1** show a high degree of orientation selection in terms of modulation frequency and modulation depth (Fig. 4a). Fourier transforming the PELDOR time traces gives a clear qualitative picture of the orientations of the nitroxides relative to the vector connecting the spin centres. The *XX* experiment shows the largest selection of the parallel dipolar component ($\theta = 0°$) while the *ZZ* experiment shows the largest perpendicular dipolar component ($\theta = 90°$). This implies that the orientation of the g_x tensor component is largely parallel and the g_{zz} component perpendicular to the molecular backbone/dipolar distance vector. This necessarily means that the orientation of the g_x tensor component on one nitroxide (spin *A*) (Fig. 3, inset) is largely perpendicular to the g_{zz} tensor component of the other nitroxide within the same molecule (spin *B*). This is supported by the very small modulation in the *ZX* time trace.

To obtain a more quantitative picture of the mutual orientation of the nitroxide spin labels and the inherent conformational flexibility of the molecule the PELDOR time traces were simulated with a home-written Matlab® program based on an approach published by the Prisner lab [23]. In a first step, a geometry optimised structure of **1** was obtained from density functional theory (DFT) calculations. The lengths of the molecular linker and nitroxide moieties obtained from that structure were then used as initial geometric values to construct a vector model where each nitroxide including the ester groups and the connecting bridge were represented by three independent vectors (Fig. 5a).

The two nitroxides groups in **1** were allowed to rotate freely around the phenolic bond with the N–O bond (g_{xx} tensor component) tracing out a cone with a mean opening of 25° and the g_{zz} and g_{yy} tensor components having a random position in the

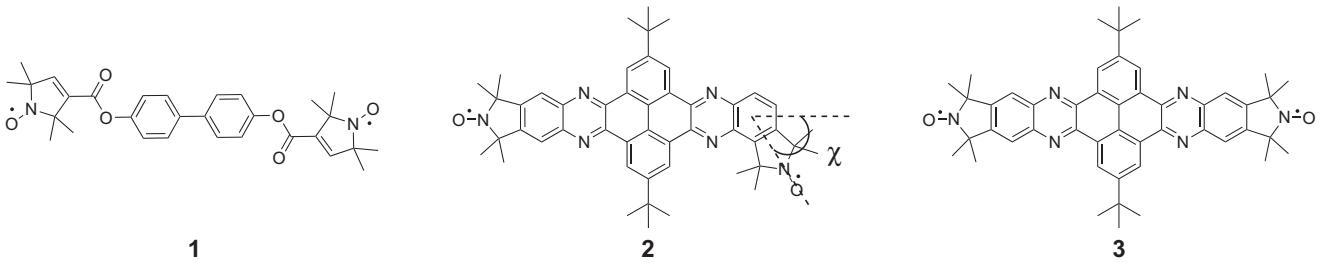

Fig. 1. Structure of nitroxide biradicals **1**–**3**. For **2**, χ denotes the angle between the nitroxide g_x components. Their synthesis is described elsewhere [13,22].

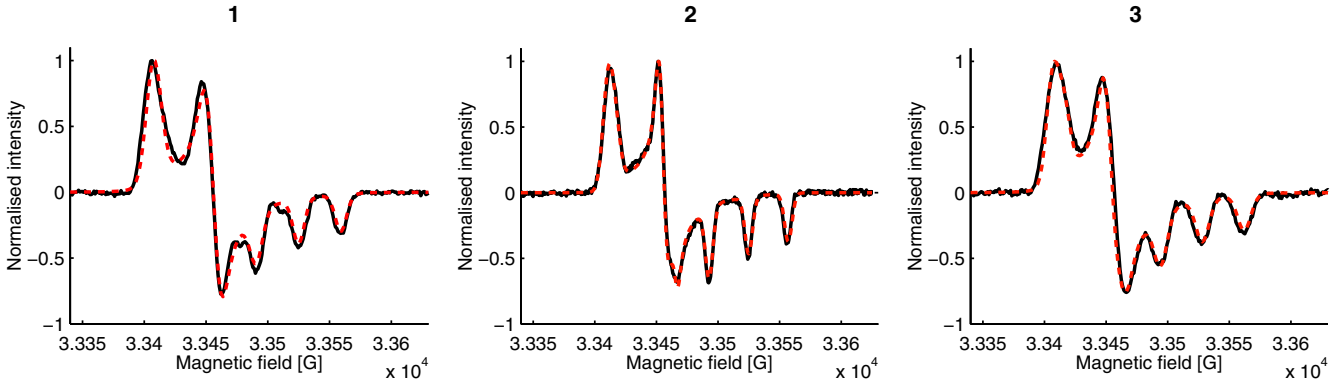

Fig. 2. W-band CW-EPR spectra of **1**, **2** and **3** at 110 K (solid black) with simulations overlaid (dashed red). (For interpretation of the references to colour in this figure legend, the reader is referred to the web version of this article.)

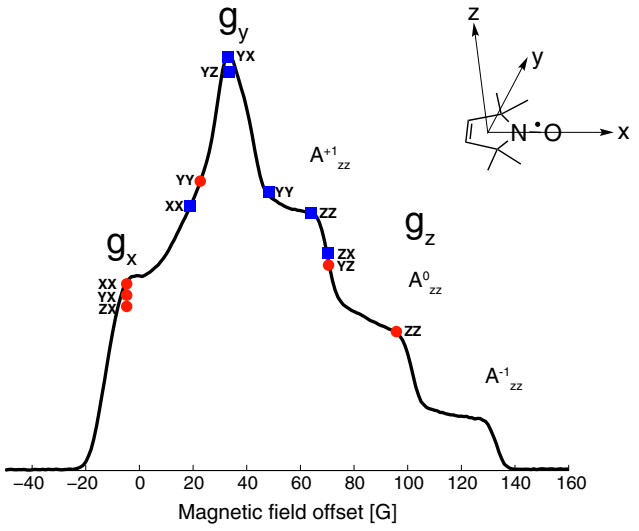

Fig. 3. An echo detected field sweep of **1**. Red dots and blue squares show the positions of the detection and inversion pulses, respectively. The dots and squares are labelled with their respective PELDOR experiment. The inset shows a nitroxide and the relative orientation of the *g*-tensor indicated by arrows. (For interpretation of the references to colour in this figure legend, the reader is referred to the web version of this article.)

zy-plane. The flexibility in the molecular linker was modelled with a single normal distributed bending motion about the biphenyl bond (Fig. 5a). From this ensemble of conformers the intramolecular interspin distance distribution was obtained by measuring the distance between the nitroxide spin centres (defined as the centre of the N–O bond) for each generated molecular conformer. The PELDOR time traces were simulated using the spin-Hamiltonian parameters obtained from the simulation of the CW-EPR spectrum of **1** (Fig. 2a) and the geometrical parameters. The cone angle (α) and degree of molecular linker flexibility (β) were iterated until one set of parameters gave good fits to all six time traces. The structural parameters yielding simulations with the best fit to the experimental time traces (Fig. 4a) are summarised in Table 1. The mean distance of 19.3 Å agrees well with the 19.8 Å obtained from the geometry optimised structure. The cone angle and linker flexibility are in good agreement with previous X-band PELDOR studies on analogues biradical systems [12,13,23]. We were not able to find another set of geometric parameters that were able to fit all six time traces at the same time. We therefore believe that this is a unique solution.

If there is negligible correlation between the orientation of coupled spin centres, the distance distribution is easily obtained by inverting the time-domain data into the distance-domain using Tikhonov regularization, as implemented into DeerAnalysis [24]. However, the time traces here show strong orientation selection indicating strong correlations, which means they cannot be treated individually in DeerAnalysis. In such a case summing up the time traces yields a good approximation to an orientation averaged time trace [25], which may be analysed in DeerAnalysis. This is shown in Fig. 4c for bisnitroxide **1**. The distance distribution agrees very well with the simulated distance distribution from the molecular conformer ensemble apart from a small broad peak in the range 15–17 Å. These smaller distances would correspond to unlikely molecular conformers and are rather artefacts due to incomplete orientation averaging.

2.2. Biradical *2* and *3*

Biradicals **2** and **3** [22] were recorded with PELDOR at approximately the same field positions as for **1** (Fig. 4d and g). The set of PELDOR time traces for **2** show a large difference in modulation frequency and depth between field positions. The largest orientation correlations are seen in the *XX*, *ZZ* and *YX* experiments (Fig. 4d). From the Fourier transformed time traces it is seen that the *XX* and *YX* experiment show an intense parallel dipolar component and the *ZZ* experiment an intense perpendicular component (Fig. 4e). This immediately suggests that the g_x and g_y tensor components are more parallel than perpendicular to the molecular backbone and the g_z tensor components are largely perpendicular to the molecular backbone. However, care must be taken in the detailed interpretation as the time traces also show that the relative modulation frequencies of the parallel and perpendicular components are clearly not consistent with a simple dipolar model, where $\nu_{||} = 2\nu_{\perp}$ suggesting that it is necessary to include an exchange coupling term in the analysis [19].

Thus, to obtain the interspin distance distribution and the relative orientation of the nitroxides from the PELDOR data, the PELDOR time traces were again simulated by using the Hamiltonian parameters obtained from the simulation of the CW-EPR spectrum of **2** (Fig. 2), a geometry model and in addition by taking into account an exchange coupling constant, *J* (Fig. 4d). As was done for **1**, distances and angles were obtained from a geometry optimised structure of **2** (Fig. 1) and substituted as initial mean values into a simple vector model (Fig. 5b). In the vector model one nitroxide was aligned such that its g_x tensor component was parallel to the molecular backbone and the g_x and g_y tensor components of the other nitroxide were rotated 60° about its g_z tensor component.

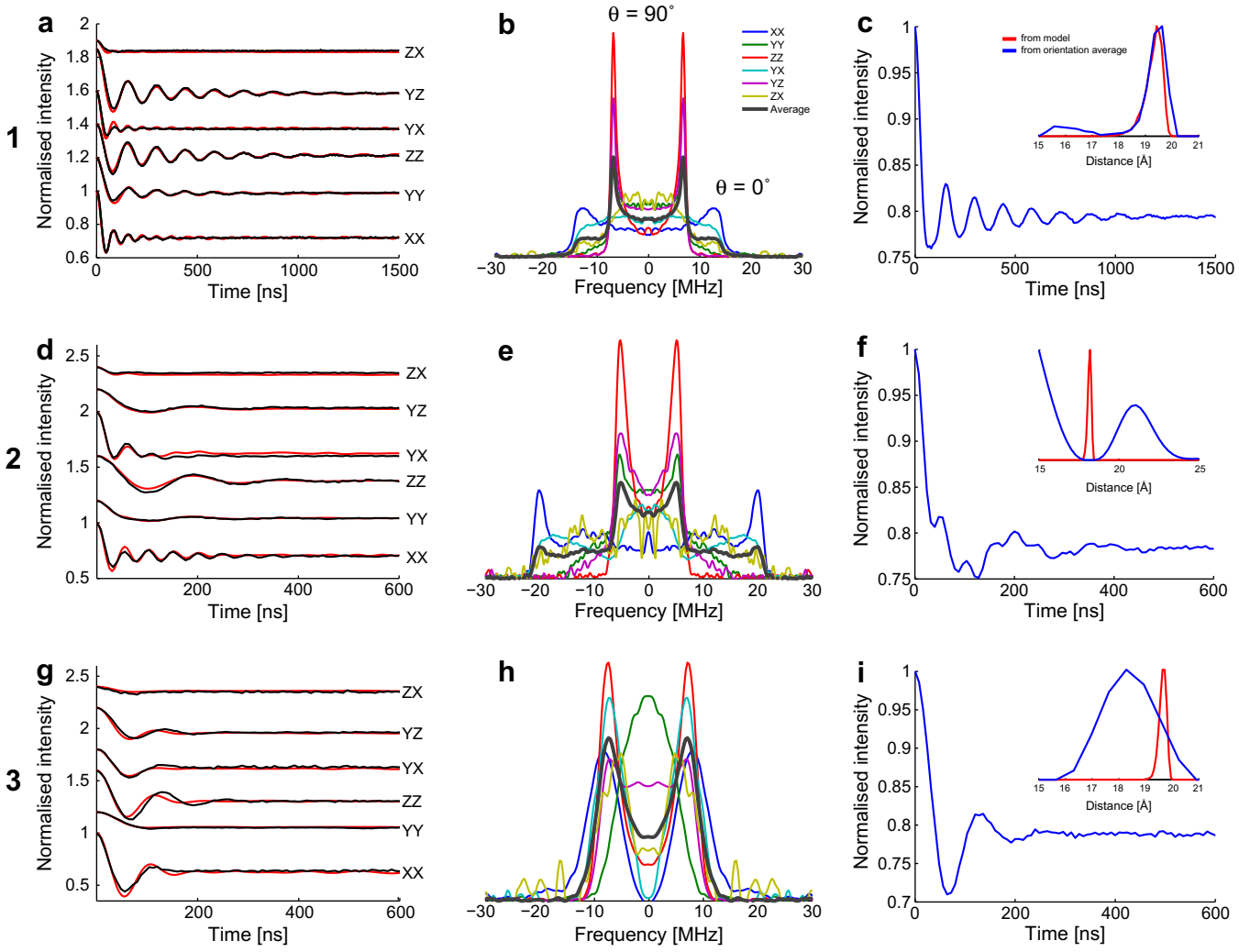

Fig. 4. PELDOR data for compounds **1**–**3**. (a, d, and g) Background corrected time traces (black) with simulated time traces overlaid (red). *ZX* denotes inversion pulse on g_z and detection sequence on g_x, etc. The time traces are displaced on the *y*-axis for clarity. (b, e, and h) Fourier transformed spectra of the six individual time traces, plus the Fourier transformation of their sum (black line). (c, f, and i) Sum of all time traces and distance distribution from simulation (red) and summed time trace (blue).

The molecular backbone, that now also includes the nitroxide moiety, was allowed to have a discrete bending in the *zx* plane about the centre of the molecule, described with a normal distribution. Bending of such molecules has also been observed in X-ray crystallographic analysis of analogous compounds [26]. Including an exchange coupling of -3.2 ± 0.8 MHz and a discrete molecular bending of ±10° with a distribution of 2.5° resulted in the best fit to the experimental PELDOR time traces. The exchange coupling is in excellent agreement with the value determined from the X-band PELDOR data [22]. Including a discrete molecular bending was necessary in order to simulate the observed modulation depth of all six time traces of **2** and indeed also of **3** (see below). In the X-band study [22] a bending of ±5° was added to rectify the distribution in *J*, which was required to fit the damping of the time traces. The higher degree of orientation selection at W-band and the possibility to probe different orientation correlations with HiPER verifies and gives a more quantitative picture of this mode. The simulated distance distribution has a mean distance of 18.04 Å with a width of 0.26 Å, in agreement with the distance from the geometry optimised structure (Table 1).

It is interesting to note that at X-band, for molecule **2**, it was difficult to distinguish between two sets of solutions for *r* and *J* even via simulations [22]. The HiPER PELDOR time traces for **2** were therefore simulated with both of these solution sets. While one solution set agrees with the values used for the simulation in Fig. 4d, the other has an exchange coupling constant of −10.5 MHz and an interspin distance of 20.7 Å [22]. Using the latter set as values for the distance and exchange coupling did not result in simulations with good fits to any of the six time traces (Fig. 6). Therefore, the higher degree of orientation selectivity at W-band makes it easier to determine a unique set of values for the exchange coupling and interspin distance.

Summing up all the experimental time traces for **2** and analysing the orientation averaged time trace with DeerAnalysis yields a broad distance distribution with two major distances. Neither of which agrees with the simulated distance nor represent a realistic molecular conformer (Fig. 4f). The discrepancy between the distance distributions is caused by the inherent exchange coupling which is not accounted for in DeerAnalysis.

The PELDOR time traces of **3** were simulated using the Spin Hamiltonian parameters obtained from cw EPR simulations and using the same vector model and dynamics that were used to simulate the PELDOR time traces of **2** with the exception that the two nitroxide g_x tensor components are antiparallel (Fig. 1). Including

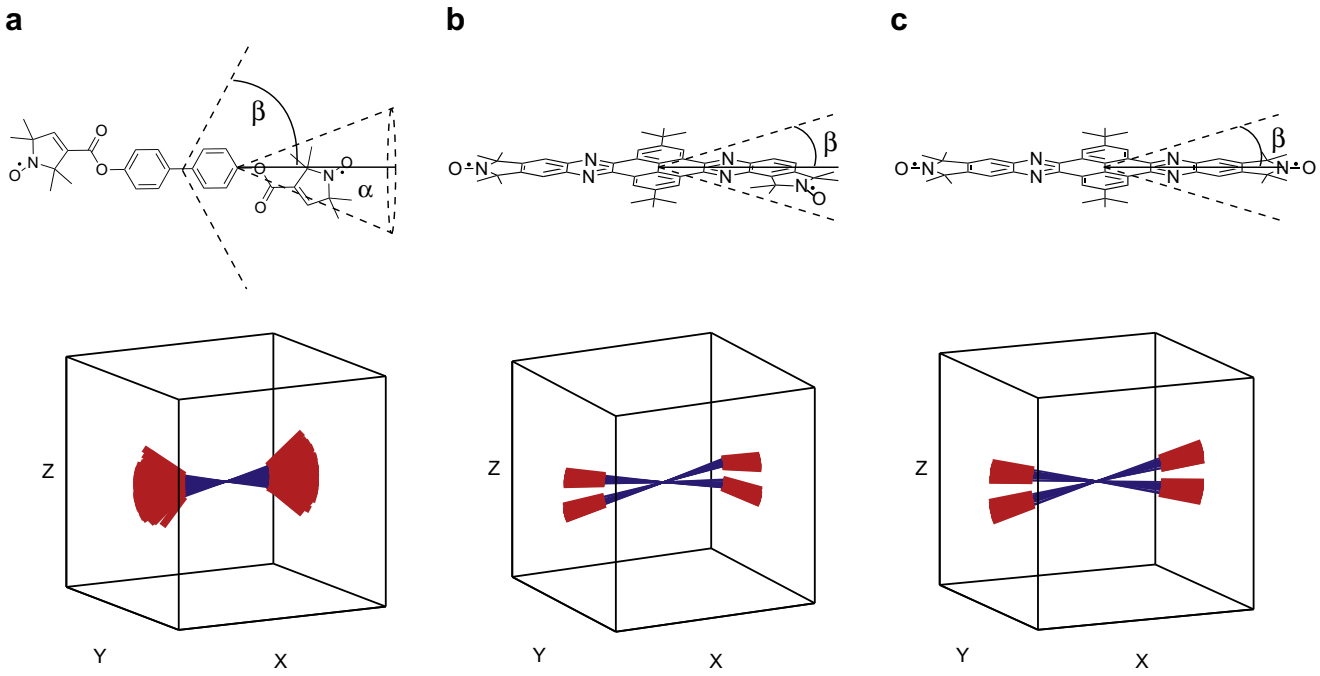

Fig. 5. (a–c) Structures and corresponding geometrical vector models used in the simulation program for biradicals **1**–**3**, respectively. Blue lines represent the connecting bridge. Red lines represent the nitroxide moieties including the ester groups. Each model shows the conformations of 20 conformers. The molecular flexibility is described by the backbone bending angle β and the cone angle α, describing the flexibility of the nitroxide moiety. (For interpretation of the references to colour in this figure legend, the reader is referred to the web version of this article.)

Table 1
Structural parameters determined from DFT calculations, PELDOR measurements and simulations.

Biradical	r_{DFT} (Å)[a]	r_{PELDOR} (Å)[b]	α (°)[c]	β (°)[d]	χ (°)[e]
1	19.8	19.30, 0.34 (0.15, 0.01)	25, 5 (3, 2.5)	0, 5 (5, 2.5)	–
2	18.4	18.04, 0.13 (0.03, 0.01)	–	10, 2.5 (4, 1.4)	60
3	20	19.70, 0.15 (0.03, 0.01)	–	10, 2.5 (3, 1.5)	0

[a] Interspin distances obtained from DFT calculations. The interspin distance was measured between the centres of the NO bonds.
[b] The distance distribution obtained by simulation of the PELDOR time traces is represented as a mean value, standard deviation. The error in the mean value and standard deviation is in brackets. The width of the distance distribution is defined as two times the standard deviation.
[c] The angle of the cone α is given as a normal distribution with mean value, standard deviation. The error in the mean value and standard deviation is in brackets.
[d] The bending of the backbone β is given as a normal distribution with mean value, standard deviation. The error in the mean value and standard deviation is in brackets.
[e] For **3**, the angle between the g_x components χ is defined as 0°.

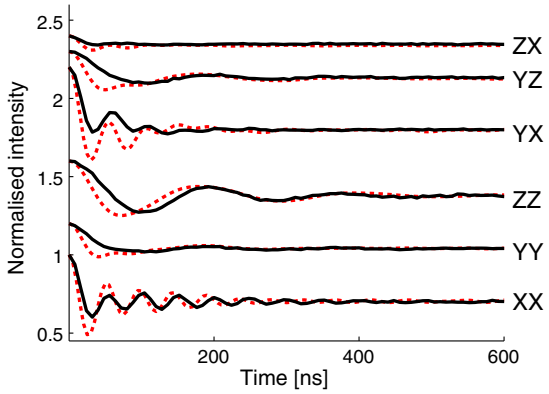

Fig. 6. Experimental (solid black) and simulated (dashed red) time traces for bisnitroxide **2**. The simulated time traces were calculated using an interspin distance of 20.7 Å and exchange coupling of −10.5 MHz. (For interpretation of the references to colour in this figure legend, the reader is referred to the web version of this article.)

an exchange coupling constant of 2.5 ± 1.7, as determined from the X-band data [22], resulted in the best overall fit to the experimental data (Fig. 4g). The simulated distance distribution obtained from the conformational ensemble has a mean value of 19.7 Å and a width of 0.3 Å, which agrees with the distance from the DFT geometry optimised structure of **3** (Table 1). In contrast, analysing the orientation averaged time trace of **3** gives a single distance with a broad distribution that does not agree with the simulated distance distribution (Fig. 4i) due to the inherent exchange coupling which is not accounted for in DeerAnalysis.

In contrast to biradical **2** the PELDOR time traces for **3** do not show a large difference in modulation frequency (Fig. 4g). This is also revealed in the Fourier transformed time traces that do not show a clear distinction between the parallel and perpendicular dipolar components (Fig. 4h). At X-band, this was also observed and is attributed to the parallel and perpendicular component of the dipolar tensor coinciding due to the presence of an exchange coupling constant [22]. At X-band it was therefore not possible to distinguish between solutions for r and J via simulations [22]. One set of solutions had r approaching infinity and $J = \pm 8.3$ MHz and the other solution had values used for the simulation in Fig. 4g. Using an interspin distance of 10 m (as an approximation for infinity) and an exchange coupling of ±8.3 MHz as initial values for the simulations of the HiPER PELDOR time traces resulted in worse fits, particularly for *YY* and *YZ* (Fig. 7).

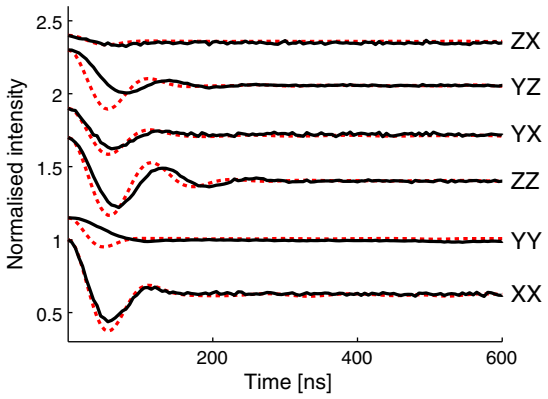

Fig. 7. Experimental (solid black) and simulated (dashed red) time traces for bisnitroxide **3**. The simulated time traces were done using an interspin distance of 10 m and an isotropic exchange coupling of 8.5 MHz (−8.5 MHz gives identical solutions). (For interpretation of the references to colour in this figure legend, the reader is referred to the web version of this article.)

As for **2** the higher degree of orientation selection at W-band makes it possible to determine a unique set of values for the exchange coupling and interspin distance.

3. Conclusions

We have shown that it is possible to make high sensitivity orientation dependent PELDOR measurements at W-band and quantitatively model the data sets to provide accurate information on the relative orientation and molecular flexibility of semi-rigid and exchange coupled rigid biradicals. The conformational flexibility of the nitroxide spin labels and the molecular linker measured for biradicals **1** were in good agreement with parameters obtained from X-band PELDOR on structurally analogous biradicals [12,23]. From the W-band PELDOR data it became possible to quantitatively determine the relative orientation of the spin labels for **2** and **3**. Specifically, the change in the orientation of the g_x and g_y tensor components between **2** and **3** was resolved, which was not possible at X-band [22]. In addition, the conformational distribution of the molecular linker in biradical **2** and **3** was quantitatively determined with less ambiguity than at X-band [22]. By simulating the W-band PELDOR time traces it became possible to unravel the exchange coupling from the PELDOR time traces and to more easily determine a unique set of solutions for the interspin distances and exchange couplings [22]. We have shown that acquiring PELDOR with the HiPER spectrometer, which gives the possibility to probe the correlation between all principal *g*-tensor components, makes it possible to acquire a detailed picture of spin label orientation and conformational flexibility on a set of semi-rigid and rigid nitroxide biradicals. The results presented in this study set the stage for structural determination on biological systems from measurements of distances, orientations and dynamics using high power, wideband, W-band spectrometers and simulations.

4. Experimental

4.1. Sample preparation

Biradical **1** (100 μM) was dissolved in molten d14 o-terphenyl obtained from Chem Service (98%C). The synthesis of **1** has been described elsewhere [13]. Biradicals **2** and **3** (100 μM) were dissolved in d-8 toluene obtained from Cambridge Isotope Laboratories Incorporation (99.5%). The samples (~50 μL) were shock-frozen in liquid nitrogen before loading into the spectrometer. The synthesis of **2** and **3** have been described elsewhere [22].

4.2. Pulse EPR measurements

Pulse EPR measurements were recorded using a home-built W-band EPR spectrometer using a non-resonant sample holder operating in reflection and induction mode, which has been described before [21]. All frequency, phase and pulse control of both inversion and detection frequencies is performed at frequencies near 7.8 GHz, before multiplication to 94 GHz and amplification to beyond 1 kW. The frequency of both low noise inversion and detection pulse sources may be separately phase locked at any frequency within a 1 GHz bandwidth at W-band, which allows complete coverage of the nitroxide spectrum. Phase coherent, heterodyne detection of the detection pulse frequency is performed with an IF frequency of 1800 MHz, with excellent electronic phase stability. The inversion pulse source is not phase related to the local oscillator. High power amplification is performed using an Extended Interaction Klystron Amplifier (EIKA) (CPI, Communications & Power Industries) operating at 94 GHz with a 1 GHz instantaneous bandwidth. Power is transmitted to the sample and to the detector through low loss quasi-optics, where free space isolators provide >90 dB isolation between source and sample and >70 dB isolation between sample and detector. The sample is contained in a 3 mm OD, 2.5 mm ID quartz tube that is placed within a non-resonant sample holder that is designed to be pre-cooled and permit cold sample loading. High isolation (>40 dB) between source and detector is maintained by operating in induction mode. The sample is irradiated by a single linear polarisation and the orthogonal polarisation is detected. This technique also allows conventional, very fast (ns), low power (few Watt) switches to be used for receiver protection. For measurements at cryogenic temperatures a continuous flow helium cryostat (CF935) and a temperature control system (ITC 502) from Oxford instruments were used. All pulsed experiments were performed at 50 K. The PELDOR experiments were done using the four pulse sequence, $\pi/2(\nu A) - \tau 1 - \pi(\nu A) - (\tau 1 + t) - \pi(\nu B) - (\tau 2 - t) - \pi(\nu A) - \tau 2 - echo$. The length of the $\pi/2$ and π detection pulses (νA) were 8 and 16 ns respectively. The length of the inversion pulse (νB) varied between 14 and 21 ns, depending on sample and field position. The time delay between the first two detection pulses (d1) was set to 300 ns. The inversion pulse position was incremented by 5 ns. The sequence repetition rate was 2.5 kHz with 3000 shots per point. Interferences from ^{14}N nuclear modulations, which might be expected and that would show up predominately at the end of the time trace, were not discernible in neither the PELDOR time traces nor the Fourier transformed time traces, and indeed have not yet been seen in any PELDOR experiments using this instrumentation. Each PELDOR time trace for biradicals **1**, **2** and **3** was measured in approximately 30 min.

4.3. Data analysis and simulations

A three dimensional homogeneous background model was fitted and subtracted from the experimental PELDOR time traces using DeerAnalysis 2011. The starting time for the background fit was adjusted to minimise any singularity in the dipolar spectrum at zero frequency. The orientation averaged PELDOR time traces were constructed by normalising the original time traces and summing them up. This is also a common strategy for orientation selected NMR residual dipolar coupling patterns [27].

4.4. Molecular modelling

Geometry optimised structures of biradicals **1**–**3** were obtained using density functional theory (DFT) as implemented in the program Orca [28]. DFT calculations were done using the B3LYP functional and 6-31G* basis set [29].

4.5. CW-EPR simulations

The W-band CW-EPR spectra recorded of **1**–**3** were simulated using the program EasySpin [30]. All spectra were simulated without including dipolar or exchange couplings. The parameters obtained from the simulations are listed in Table 2.

4.6. PELDOR simulations

PELDOR time traces were simulated with a home-written Matlab® program. A laboratory frame (*X*, *Y*, *Z*) is defined, with the applied magnetic field B_0 aligned along the *Z*-axis. Within this frame the geometry of the biradicals were represented by a vector model from which the distance vector is calculated (Fig. 8).

Orientation of the *g*- and hyperfine-tensors are defined relative to this distance vector. The conformational dynamics of the molecules were represented by creating 20,000 different molecular conformers employing a simple dynamics model including backbone bending about the midpoint and rotation of the nitroxides on a cone [23]. The relative orientations of spin labels and the interspin vector were calculated for each conformer. The interspin distance vector **r** for each conformer was given a $\sin(\theta)$ weighted random orientation on the half sphere with respect to the laboratory frame and the orientation of the *g*- and hyperfine-tensors relative to the laboratory frame calculated. The *g*- and hyperfine-tensors were assumed to be collinear.

The resonance frequencies for each spin centre were computed from the respective orientations, the *g*-tensor values, ^{14}N hyperfine coupling values and line width. Calculating the frequencies for each of the ^{14}N nuclear spin quantum number m_I yields a total of 120,000 single spin centres.

The excitation profiles for the detection $I_{\nu 1}$ and inversion $I_{\nu 2}$ pulses are described by Eqs. (1) and (2) respectively [31],

$$\begin{aligned} I_{\nu 1} &= \frac{\xi}{\zeta}\sin(\zeta t_{\pi/2})\frac{\xi'^4}{4\zeta'^4}[1-\cos(\zeta' t_\pi)]^2 \\ \xi &= \frac{\pi/2}{t_{\pi/2}} \\ \xi' &= \frac{\pi}{t_\pi} \\ \zeta^2 &= \xi^2 + (\omega-\omega_r)^2 \\ \zeta'^2 &= \xi'^2 + (\omega-\omega_r)^2 \end{aligned} \tag{1}$$

$$I_{\nu 2} = \frac{\xi'^2}{2\zeta'^2}[1-\cos(\zeta' t_\pi)] \tag{2}$$

where $(\omega-\omega_r)$ is the frequency offset of the microwave pulses. The lengths of the $\pi/2$ and π pulses are given by $t_{\pi/2}$ and t_π, respectively.

The contribution from each spin pair to the PELDOR modulation is then computed from the detection of spin *A* weighted by the inversion probability of spin *B* and the detection of spin *B* weighted by the inversion probability of spin *A* (Eq. (3)). The degree of PELDOR modulation for each spin pair depends on the angle between the interspin vector and the applied magnetic field θ, the set of Euler angles that describe the orientation of the *g*- and *A*-tensors φ and the detection and inversion pulse frequencies, ν_1 and ν_2 respectively.

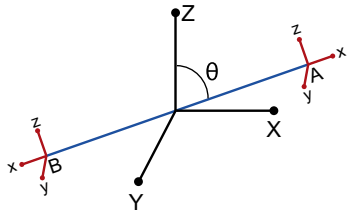

Fig. 8. A vector diagram showing the laboratory frame (*X*, *Y*, *Z*) and the frames of two connected spin centres *A* and *B*. The interspin distance is depicted by a blue line with the angle to the applied magnetic field represented by θ.

$$\begin{aligned} \Psi(\theta,\varphi_A,\varphi_B,\nu_1,\nu_2) = {} & I_{\nu 1}(A)(1-I_{\nu 2}(A))I_{\nu 2}(B)(1-I_{\nu 1}(B)) \\ & + I_{\nu 1}(B)(1-I_{\nu 2}B)I_{\nu 2}(A)(1-I_{\nu 1}(A)) \end{aligned} \tag{3}$$

$I_{\nu 1}(A)$ represents excitation of spin *A* by the detection sequence. The excitation of spin *A* is weighted by the excitation of spin *B* by the inversion pulse, $I_{\nu 2}(B)$. In case of pulse overlap the detection of spin *A* and inversion of spin *B* are weighted by the inversion probability of spin *A* and detection probability of spin *B*, $(1-I_{\nu 2}(A))$ and $(1-I_{\nu 1}(B))$ respectively.

Likewise, the intensity of the echo produced by the detection sequence without the inversion pulse is computed by Eq. (4), where *N* is the number of molecular conformers.

$$V_0 = \sum_{i=1}^{N} I_{\nu 1}(A) + I_{\nu 1}(B) \tag{4}$$

For *N* spin pairs, each with a finite number *R* of orientations, the intensity of the refocused echo *V* with the position of the inversion pulse *T* can be described by Eq. (5).

$$V(T) = V_0 + \sum_{i=1}^{N}\sum^{R} \Psi^i[\cos(DT)-1] \tag{5}$$

D is the dipolar coupling

$$D = \frac{\mu_o g^2 \beta_e^2}{4\pi\hbar}\frac{1}{r_i^3}(1-3\cos^2(\theta)) + J \tag{6}$$

where μ_0 is the permeability of vacuum, *g* the isotropic *g*-value, β the Bohr magneton, $\hbar$ the reduced Planck constant, *r* the interspin distance and *J* the isotropic exchange coupling constant.

By computing V_0 and Ψ, θ and *r* for each molecular conformer and using Eq. (5) the PELDOR time trace is constructed. The calculations of six time traces from 20,000 conformers takes about 14 s

Table 2
Parameters used for the simulations of the cw EPR spectra of compounds **1**–**3**.

Parameters	**1**	**2**	**3**
g_{xx}, g_{yy}, g_{zz}	2.0104, 2.0073, 2.0033	2.01, 2.0072, 2.0033	2.0101, 2.0073, 2.0031
g-Strain[a]	0.0004, 0.0003, 0.0001	0.0005, 0.0002, 0.0003	0.0003, 0.0003, 0.0005
A_{xx}, A_{yy}, A_{zz}[b]	8, 6, 96	10, 12, 90	16, 13, 95
A-strain[c]	0, 0, 12	5, 0, 5	1, 1, 5
Linewidth[d]	0.8, 0.13	0.4, 0.02	0.7, 0.11

[a] The *g*-strain is given in MHz and listed in the following order (*x*, *y*, *z*).
[b] The ^{14}N hyperfine coupling values are in MHz.
[c] The *A*-strain is given in MHz and listed in the following order (*x*, *y*, *z*).
[d] The linewidths (Gaussian, Lorentzian) is the peak to peak linewidth in mT.

to compute on a 2.8 GHz Intel processor. The uncertainty in simulation parameters was assessed qualitatively by varying each simulation parameter individually. The difference in a parameter value giving noticeably different simulations was assigned as the error for that variable.

Acknowledgments

This work was supported by the BBSRC (Grant No. BB/H017917/1), the EPSRC (Grant No. F004583/1) and the Icelandic Research Fund (60028021). G.W.R. acknowledges the School of Biology, University of St Andrews for a SORS (Scottish Overseas Research Students) Scholarship and O.S. thanks the Research Councils of the UK for an RCUK fellowship.

Appendix A. Supplementary material

Supplementary data associated with this article can be found, in the online version, at doi:10.1016/j.jmr.2012.01.019.

References

[1] R.E. Martin, M. Pannier, F. Diederich, V. Gramlich, M. Hubrich, H.W. Spiess, Determination of end-to-end distances in a series of TEMPO diradicals of up to 2.8 nm length with a new four-pulse double electron electron resonance experiment, Angew. Chem., Int. Ed. 37 (1998) 2833–2837.
[2] A.D. Milov, K.M. Salikhov, M.D. Shirov, Application of the double resonance method to electron spin echo in a study of the spatial distribution of paramagnetic centers in solids, Sov. Phys. – Solid State 23 (1981) 565–569.
[3] G.W. Reginsson, O. Schiemann, Pulsed electron–electron double resonance: beyond nanometre distance measurements on biomacromolecules, Biochem. J. 434 (2011) 353–363.
[4] G.W. Reginsson, O. Schiemann, Studying biomolecular complexes with pulsed electron–electron double resonance spectroscopy, Biochem. Soc. Trans. 39 (2011) 128–139.
[5] G. Jeschke, Y. Polyhach, Distance measurements on spin-labelled biomacromolecules by pulsed electron paramagnetic resonance, Phys. Chem. Chem. Phys. 9 (2007) 1895–1910.
[6] V.P. Denysenkov, T.F. Prisner, J. Stubbe, M. Bennati, High-field pulsed electron–electron double resonance spectroscopy to determine the orientation of the tyrosyl radicals in ribonucleotide reductase, Proc. Natl. Acad. Sci. 103 (2006) 13386–13390.
[7] Y. Polyhach, A. Godt, C. Bauer, G. Jeschke, Spin pair geometry revealed by high-field DEER in the presence of conformational distributions, J. Magn. Reson. 185 (2007) 118–129.
[8] O. Schiemann, P. Cekan, D. Margraf, T.F. Prisner, S.T. Sigurdsson, Relative orientation of rigid nitroxides by PELDOR: beyond distance measurements in nucleic acids, Angew. Chem., Int. Ed. 48 (2009) 3292–3295.
[9] A. Marko, D. Margraf, P. Cekan, S.T. Sigurdsson, O. Schiemann, T. Prisner, Analytical method to determine the orientation of rigid spin labels in DNA, Phys. Rev. E 81 (2010) 021911-1–021911-9.
[10] A. Marko, V.P. Denysenkov, D. Margraf, P. Cekan, O. Schiemann, S.T. Sigurdsson, T. Prisner, Conformational flexibility of DNA, J. Am. Chem. Soc. 133 (2011) 13375–13379.
[11] B. Endeward, J.A. Butterwick, R. MacKinnon, T. Prisner, Pulsed electron–electron double-resonance determination of spin-label distances and orientations on the tetrameric potassium ion channel KcsA, J. Am. Chem. Soc. 131 (2009) 15246–15250.
[12] B.E. Bode, J. Plackmeyer, M. Bolte, T. Prisner, O. Schiemann, PELDOR on an exchange coupled nitroxide copper(II) spin pair, J. Organomet. Chem. 694 (2009) 1172–1179.
[13] B.E. Bode, J. Plackmeyer, T.F. Prisner, O. Schiemann, PELDOR measurements on a nitroxide-labeled Cu(II) porphyrin: orientation selection, spin-density distribution, and conformational flexibility, J. Phys. Chem. A 112 (2008) 5064–5073.
[14] D.M. Bridges, K. Hideg, W.L. Hubbell, Resolving conformational and rotameric exchange in spin labeled proteins using saturation recovery EPR, Appl. Magn. Reson. 37 (2010) 363–390.
[15] M.R. Fleissner, D.M. Bridges, E.K. Brooks, D. Cascio, T. Kálai, K. Hideg, W.L. Hubbell, Structure and dynamics of a conformationally constrained nitroxide side chain and applications in EPR spectroscopy, Proc. Natl. Acad. Sci. U. S. A. 108 (2011) 16241–16246.
[16] I. Tkach, G. Sicoli, C. Höbartner, M. Bennati, A dual-mode microwave resonator for double electron–electron spin resonance spectroscopy at W-band microwave frequencies, J. Magn. Reson. 209 (2011) 341–346.
[17] A. Savitsky, A.A. Dubinskii, M. Flores, W. Lubitz, K. Möbius, Orientation-resolving pulsed electron dipolar high-field EPR spectroscopy on disordered solids: I. Structure of spin-correlated radical pairs in bacterial photosynthetic reaction centers, J. Phys. Chem. B 111 (2007) 6245–6262.
[18] M. Flores, A. Savitsky, M.L. Paddock, E.C. Abresch, A. Dubinskii, M.Y. Okamura, W. Lubitz, K. Möbius, Electron-nuclear and electron-electron double resonance spectroscopies show that the primary quinone acceptor QA in reaction centers from photosynthetic bacteria *Rhodobacter sphaeroides* remains in the same orientation upon light-induced reduction, J. Phys. Chem. B 114 (2010) 16894–16901.
[19] V.P. Denysenkov, D. Biglino, W. Lubitz, T. Prisner, M. Bennati, Structure of the tyrosyl biradical in mouse R2 ribonuleotide reductase from high-field PELDOR, Angew. Chem. 47 (2008) 1224–1227.
[20] D. Goldfarb, Y. Lipkin, A. Potapov, Y. Gorodetsky, B. Epel, A.M. Raitsimring, M. Radoul, I. Kaminker, HYSCORE and DEER with an upgraded 95 GHz pulse EPR spectrometer, J. Magn. Reson. 194 (2008) 8–15.
[21] P.A.S. Cruickshank, D.R. Bolton, D.A. Robertson, R.I. Hunter, R.J. Wylde, G.M. Smith, A kilowatt pulsed 94 GHz electron paramagnetic resonance spectrometer with high concentration sensitivity, high instantaneous bandwidth, and low dead time, Rev. Sci. Instrum. 80 (2009) 103102-1–103102-15.
[22] D. Margraf, P. Cekan, T. Prisner, S.T. Sigurdsson, O. Schiemann, Ferro- and antiferromagnetic exchange coupling constants in PELDOR spectra, Phys. Chem. Chem. Phys. 11 (2009) 6708–6714.
[23] D. Margraf, B.E. Bode, A. Marco, O. Schiemann, T.F. Prisner, Conformational flexibility of nitroxide biradicals determined by X-band PELDOR experiments, Mol. Phys. 105 (2007) 2153–2160.
[24] G. Jeschke, I.P. Chechik, A. Godt, H. Zimmermann, J. Banham, C.R. Timmel, J.H. Hilger, DeerAnalysis 2006 – a comprehensive software package for analyzing pulsed ELDOR data, Appl. Magn. Reson. 30 (2006) (2006) 473–498.
[25] A. Godt, M. Schulte, H. Zimmermann, G. Jeschke, How flexible are poly(paraphenyleneethynylene)s?, Angew Chem., Int. Ed. 45 (2006) 7560–7564.
[26] B. Gao, M. Wang, Y. Cheng, L. Wnag, X. Jing, F. Wang, Pyrazine-containing acene-type molecular ribbons with up to 16 rectilinearly arranged fused aromatic rings, J. Am. Chem. Soc. 130 (2008) 8297–8306.
[27] S.E. Ashbrook, Recent advances in solid-state NMR spectroscopy of quadrupolar nuclei, Phys. Chem. Chem. Phys. 11 (2009) 6892–6905.
[28] F. Neese, ORCA – An ab-initio, Density Functional and Semiempirical Program Package, University of Bonn, 2011.
[29] W.J. Hehre, R. Ditchfield, J.A. Pople, Self-consistent molecular orbital methods. XII. Further extensions of gaussian-type basis sets for use in molecular orbital studies of organic molecules, J. Chem. Phys. 56 (1972) 2257.
[30] S. Stoll, A. Schweiger, EasySpin, a comprehensive software package for spectral simulation and analysis in EPR, J. Magn. Reson. 178 (2006) 42–55.
[31] A. Marko, D. Margraf, H. Yu, Y. Mu, G. Stock, T. Prisner, Molecular orientation studies by pulsed electron–electron double resonance experiments, J. Chem. Phys. 130 (2009) 064102-1–064102-9.